Pure & Appl. Chem., Vol. 69, No. 8, pp. 1707–1723, 1997.
Printed in Great Britain.

INTERNATIONAL UNION OF PURE
AND APPLIED CHEMISTRY

MACROMOLECULAR DIVISION
WORKING PARTY ON STRUCTURE AND PROPERTIES OF COMMERCIAL POLYMERS*

CHARACTERIZATION OF FINITE LENGTH COMPOSITES: PART II. MECHANICAL PERFORMANCE OF INJECTION MOLDED COMPOSITES

(Technical Report)

The authors and contributing members dedicate this paper to their colleague and friend, Professor Gerhard Zachmann

Prepared for publication by

L. GLAS[1], P. S. ALLAN[2], T. VU-KHANH[3] AND A. CERVENKA[4]

[1]Shell Research S.A., Chemical Research Centre Shell, Louvain-la-Neuve, Belgium
[2]Brunel University, The Wolfson Centre for Materials Processing, Uxbridge, Middlesex, UK
[3]Université de Sherbrooke, Faculté des Sciences Appliquées, Département de Génie Mécanique, Sherbrooke (Québec), Canada
[4]Shell Research B.V., Koninklijke/Shell Laboratorium, Amsterdam, Netherlands

*Membership of the Working Party during the preparation of this report (1996–97) was as follows:

G. Ajroldi (Italy); P. S. Allan (UK); R. S. Bailey (UK); M. J. Cawood (UK); A. Cervenka (Netherlands); M. W. Darlington (UK); Y. Giraud (France); L. Glas (Belgium); F. H. J. Mauer (Sweden); D. R. Moore (UK); P. Szewczyk (Poland); T. Vu-Khanh (Canada).

Characterization of finite length fibre composites. Part II: Mechanical performance of injection moulded composites (Technical Report)

Abstract: An overview is given of the mechanical performance (stiffness, strength, toughness, creep...) of finite fibre length reinforced thermoplastics based on polypropylene and polyamide as the matrices and glass, carbon and Kevlar as the reinforcement. Different degrees of fibre orientation distribution and fibre attrition as produced by classical injection moulding and multiple-live feed moulding were evaluated. It was found that the simple test geometry used (injection moulded plaques) resembled more a complicated structure than a material. The properties measured therefore were more the complex response of a strongly anisotropic structure than simple material properties. Increased alignment of the fibres in a given direction affected all the mechanical properties, but the effect was largest for the tensile stiffness. A higher degree of fibre orientation, was not accompanied by an increase in properties related to failure (ultimate stress, K_{Ic}). The modelling of ultimate stress showed that this could be explained by the more severe fibre attrition which resulted from the forces applied to orient the fibres.

INTRODUCTION

This paper is the second from a series of six resulting from an IUPAC Working Party 4.2.1 (Structure and properties of commercial polymers) investigation aiming to establish relationships between the structure, the individual constituents and the material properties of composites based on thermoplastic matrices reinforced with finite length fibres.

Twelve composite structures have been studied, using three types of reinforcement (glass, carbon, Kevlar) and two matrices (polypropylene, polyamide). For the glass fibre reinforcement two different initial feedstock lengths (5 and 10 mm) were used. The materials used were the novel 'Verton' type of reinforced thermoplastic matrices developed by ICI.

With finite fibre length reinforced materials, the fibre orientation distribution has a profound effect on the mechanical properties of the finished part. Modifying the process conditions not only changes the fibre orientation distribution but also changes the degree of fibre attrition, reducing the initial fibre length L_0, increasing the overall number of fibres and inducing a distribution $n(L)$ in the fibre length with $L < L_0$. In this research two processing routes have been used to manufacture the test samples: classical injection moulding (STATIC MODE) and multiple-live feed injection moulding (DYNAMIC MODE).

In view of the size of this project, the number of structures and properties studied, and the complexity of the project in describing the structure and establishing the relationships with the properties measured, the outcome of this research is reported in six papers. An overview of the complete project (materials, nomenclature, moulding conditions, participating laboratories, general conclusions) can be found in reference 1. Reference 2 discusses mechanical properties measured on wafers extracted from mouldings in relation with the through thickness structure (skin-core). Structural aspects, such as the degree of fibre orientation over the test specimens and fibre attrition, are presented in reference 3. Structural information is related with the stiffness of the composites through modelling in reference 4. The melt flow properties of the composites and their effect on the composite structures obtained are described in reference 5. The objective of this paper is to present an overview of the mechanical properties of the 12 composite structures and where possible to relate the observations with the results on structural information, the nature of the individual constituents and the rheological investigation.

The following laboratories participated to this study:

Brunel University	London, UK	1
Shell Research	Louvain-la-Neuve, Belgium Arnhem, The Netherlands	2
Ausimont	Bollate, Italy	3
ICI	Wilton, UK	4
National Research Council	Montreal, Canada	5
BP	Grangemouth, UK	6
Rhone-Poulenc	Saint Fons, France	7
DSM	Geleen, The Netherlands	8
Cranfield University	Bedford, UK	9
Inst. Prezem. Tworz. i. Farb	Gliwice, Poland	10

The numbers at the end of each line are used in table 1 to identify the contribution of the laboratories to each part of the study.

To identify the composites the following code is used: XX\y nn, where XX refers to the thermoplastic matrix (PP or PA), y refers to the fibre type (g for glass, c for carbon and k for Kevlar). nn is the initial fibre feedstock length/mm (nn is 5 or 10). PP\g 10 is then a glass fibre reinforced polypropylene with an initial fibre feedstock length of 10 mm.

EXPERIMENTAL

Performance characterisation of the materials has been carried out by measuring properties on test specimens machined from the injection moulded square plaques (with dimensions 85 x 85 x 6 mm). Specimens were cut either parallel to the direction coinciding with the melt flow (yielding the longitudinal properties) or perpendicular to this direction (yielding the transverse properties). Table 1 presents an overview of the properties measured and includes the way of their determination (deformation mode and testing speed), the material-fibre combinations tested, the type of specimen used and the laboratory performing the experiment.

The **tensile modulus** at the lowest deformation speeds (0.1-1 mm/min) was measured by laboratories 1, 2 and 5, on standard testing machines with different types of extensometers. The high deformation speed (0.05-0.1 m/s) experiments were performed on an Instron Dynamometer, Model 8031, by laboratory 3. In this type of experiment the longitudinal

TABLE 1. Overview of the properties measured and the experimental methods used

Property	deformation mode	testing speed	materials	sample type(2)	data from (3)
modulus	tensile	0.1, 1 mm/min	all	DB,B	1,2,5
		0.05 m/s	PA\c 10	B	3
		0.1 m/s	all but PA\c 10	B	3
	flexural	2 mm/min	all but PA\k 10	DB	7,4
creep modulus	tensile	-	PP\g 5, PP\g 10, PA\g 5, PA\g 10	B	9
	flexural	-	all but PA\c 10	B	3
relaxation modulus(1)	tensile	-	PP\g 5, PP\g 10	DB	8
rebound modulus	flexural	0.2 m/s	all	DB	3
Lateral contraction ratio	tensile	0.05 m/s	PA\c 10	B	3
		0.1 m/s	all but PA\c 10	B	3
ultimate stress and strain	tensile	0.1, 1, 5 mm/min	all	DB,B	1,2,5,6,10
			PA\c 10	B	3
ultimate stress	flexural	0.05 m/s	all but PA\c 10	B	3
		0.1 m/s	all but PA\k 10	DB	7
		2 mm/min			
impact resistance	Izod		PP\g 10, PA\g 10, PA\c 10	NB	5
	disc impact	5 m/s	all but PA\c 10	CP	3
K_{Ic}	tensile	1 mm/min	all but PA\k 10	CTS	7
	flexural	10 mm/min	all	TPB	5,6
		1 m/s	all	TPB	3
thermal expansion	between 23 and 50°C		all but PA\k 10	C	2

(1) the relaxation modulus was measured at 25, 40, 60 and 80°C
(2) the following types of test specimens were used: dumb-bell shaped (DB), bar (B), notched bar (NB), complete plaques (CP), compact tension specimen (CTS), three point bending (TPB) and cubes (C).
(3) see Introduction for the identification of the individual laboratories

displacement was measured with an LVDT connected to the piston. The longitudinal strain was calculated from this displacement using two corrections. The first one is due to the fact that the axial displacement is measured between the clamps. An equivalent length L_e is calculated by means of the following formulas:

$$L_e = L_1 + L^*$$

with:

$$L^* = 2WR\left\{-\frac{1}{R}\left[\frac{\alpha}{2} - \left(\frac{W + 2R}{W}\right)\left(\frac{W}{W + 4R}\right)^{\frac{1}{2}}\right] \cdot \tan^{-1}\left[\left(\frac{W + 4R}{W}\right)\tan\frac{\alpha}{2}\right]\right\}$$

where:

W = specimen width
R = radius of curvature
α = connection angle
L_1 = constant width length

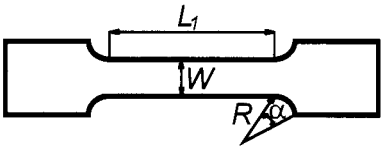

The second correction takes into account the machine compliance via the formula:

$$\Delta L(P) = \Delta L_{tot} - PC_m$$

with $\Delta L(P)$ being the real displacement at a load P, ΔL_{tot} the total displacement, P the applied load and C_m the machine compliance.
Lateral strain was measured with an in-house developed extensometer (1μm sensitivity) attached to the specimen. From the longitudinal and lateral strain the **Lateral contraction ratio** was calculated with the following formula:

$$\text{Lateral contraction ratio} = -\frac{\varepsilon_w}{\varepsilon_L} = -\frac{\Delta W(P)}{\Delta L(P)}\cdot\frac{L}{W}$$

The **modulus by flexure** was determined by laboratory 7 and 4 in three point bending tests according to ASTM D790 (reference 6) on specimens with a width of 15 mm and a span to depth ratio of 11. For the PA\c 10 composite, the specimen width was 10 mm, the deformation speed was 1 mm/min and the span to depth ratio of 10.

The **ultimate stress and strain** were derived from the same experiments as the tensile and flexural moduli. The initial cross section was used to calculate the ultimate stress.

The **tensile creep modulus** was measured by laboratory 9 on rectangular strips (width 5.5 mm) at a stress level corresponding to a 100 second strain in the region of 0.2%. The **flexural creep modulus** was determined by laboratory 3 in three point bending tests on rectangular specimens with a width of 15 mm and a support span length of 75 mm. The maximum stress applied was 10 MPa for the PP composites and 20 MPa for the PA composites.

The **relaxation modulus,** was determined by laboratory 8 on rectangular strips with a width of 5.9 mm. All experiments were carried out on a Zwick 1474 closed loop controlled tensile tester. A strain of 0.2 % was imposed in about 0.5 seconds and the relaxation modulus was determined after 10 seconds of relaxation. The strain was measured with an accuracy of 0.05 μ m by a strain sensor (Zwick nr. 93031) clamped to the sample. Forces (typically around 300 N) were measured with a 10 kN transducer with an accuracy of 0.1 N. Using a temperature controlled oven, the experiments were performed at 25, 40, 60 and 80°C. Additional experiments at 25°C and 0.1% strain were conducted to check whether the tests were performed in the linear viscoelastic range. These experiments were repeated after a heat treatment of the samples to evaluate the influence of the state of the polypropylene matrix on the relaxation modulus (the samples were stored at 130°C for 21 hours and then cooled with a rate of 1°C/min to ambient temperature).

The **rebound modulus** (reference 7) in three point bending was determined by laboratory 3 with a 50 Joule instrumented Zwick 5105 pendulum. The rebound modulus was calculated from the material response to a hammer dropped from an angle between 2 and 3° with following equation:

$$E = \left(\frac{\pi}{t_0}\right) \cdot \frac{L^3 M}{48\, I}$$

where t_0 is the rebound time, M the hammer mass, L the specimen span and I the moment of inertia of the specimen. Measurements were carried out edge- and flatwise. In the edgewise configuration the force was exerted on the longer specimen edge and for the flatwise configuration the force was exerted on the flat surface. Differences in skin-core morphology of the composites were expected to reflect in differences between these two rebound moduli.

The impact resistance was characterised by notched Izod impact tests (laboratory 4) according to ASTM D-256 (reference 8) and by instrumented falling weight experiments on plaques (laboratory 3). For the falling weight tests, the plaques were positioned on a circular anvil with a 75 mm internal diameter and impacted at 5 m/s with a dart of 8 kg mass and a diameter of 20 mm (the total impact energy available was 100 J). The instrumented falling weight equipment used in this investigation is fully described in reference 9.

The fracture toughness (K_C) was measured in mode I. K_{Ic} was determined on compact tension specimens with an *a/w* ratio of 0.5, by laboratory 7 according to ASTM E 399 (reference 10) , and in three point bending (TPB) tests on the SENB geometry by laboratories 3, 5 and 6. All notches were sharpened by pushing a razor blade in the tip of the initial milled or saw cut. For the TPB specimens, two *a/w* ratios were used, 0.4 and 0.5. All the notches were made in the plane of the injection moulded plaques parallel to either the longitudinal or transverse direction.

The thermal expansion coefficients were measured by laboratory 2 on a Perkin Elmer Thermomechanical Analyzer 2 using cube shaped samples (6x6x6 mm), machined from the centre of the plaques. The sample, loaded with a 1 mN force, was heated at 0.5°C/min until 50°C, whereafter it was cooled to 23°C at 0.5°C/min. From the displacement during the heating from 23°C to 50°C the thermal expansion coefficient was calculated. The same sample was used to determine the thermal expansion coefficient in the longitudinal, transverse and through thickness directions. To avoid any influence of residual stresses, the samples were annealed for more than 24 hours at 80 °C, and then slowly cooled to room temperature prior to testing in the Thermomechanical Analyzer.

GENERAL OBSERVATIONS ON THE MECHANICAL PROPERTIES

Anisotropy

With finite fibre length reinforced composites, changing the processing conditions can alter the fibre orientation distribution. From a macroscopic point of view, the DYNAMIC injection moulding process aligned the fibres preferentially in the longitudinal direction of the plaques used in this study, whereas in the STATIC mode the fibres tended to become oriented in the transverse direction. For fibre reinforced plastics it is well known that the mechanical properties measured in the direction parallel to the fibres will significantly differ from those measured perpendicularly to that direction. This is also valid for the materials investigated in this study.

Table 2 presents the thermal expansion coefficients of the 10 mm glass fibre composites in the

longitudinal (Long), transverse (Trans) and through thickness (*Z*) directions. With the two processing modes, the fibre orientation was mainly in the plane of the plaques, as demonstrated by the significantly higher thermal expansion coefficients measured in the *Z* direction. This does not mean that the plaques had a homogeneous structure over their thickness. As discussed in reference 2, the results from wafer studies have shown that the mechanical properties also vary with thickness. For the in-plane properties the thermal expansion coefficient measured in the direction of dominant fibre alignment (longitudinal for the DYNAMIC mode, transverse for the STATIC mode) was lower than the thermal expansion coefficient measured in the perpendicular direction. In the DYNAMIC mode the anisotropy in properties was higher than in the STATIC mode, a direct consequence of the different fibre orientation distributions obtained by the two processing modes.

TABLE 2.Thermal expansion coefficient (1/K*10E-7) between 23°C and 50°C for the composites with 10 mm initial feedstock fibre length, *Z* denotes the through thickness direction

	dynamic mode			static mode		
	PP\g	PA\g	PA\c	PP\g	PA\g	PA\c
Long	129	169	60/64	594/677	249	320
Trans	823	740/900	820	309	180	68
Z	1163	1396	1323	1252	1939/1943	1316

A difference in anisotropy observed for the PP and PA composites produced by the STATIC mode is probably due to different skin/core thickness. The PA\g composites were found to have a thicker skin region than the PP\g composites when produced by the STATIC mode (reference 3). With the DYNAMIC processing mode both types of composites had the same skin/core thickness.

Table 3 shows that, as expected, the tensile modulus measured in the 45° direction (i.e. the direction at an angle of 45° to the longitudinal and transverse directions) is very close to the modulus measured in the direction of lowest fibre orientation (longitudinal direction for the STATIC mode, transverse direction for the DYNAMIC mode). For a further discussion on the relation between modulus and fibre orientation the reader is referred to references 3 and 4.

TABLE 3. Tensile modulus (GPa) measured in various directions for the composites with 10 mm initial fibre feedstock length (low deformation speed)

	dynamic mode			static mode		
	PP\g	PA\g	PA\k	PP\g	PA\g	PA\k
Long	13.8	12.5	5.5	5.9	8.9	5
45°	4.5	7.6	5.7	6	7.5	4.6
Trans	4.2	6.1	4.8	7.9	11.1	7

Heterogeneity

The large variations in the values quoted for the mechanical properties by the participating laboratories can not be explained by the use of different test methods. Tables 4 and 5 show that the coefficient of variation for tensile modulus and fracture toughness is on average larger than 10%.

Contributing to the large scatter is the fact that all the composites have been found to exhibit a property profile over the longitudinal and transverse direction. Data for the relaxation modulus

TABLE 4. Coefficient of variation (%) of the tensile modulus on the 10 mm fibre reinforced composites (high deformation speed). The coefficient of variation is defined as $\left(\frac{100 * \text{standard deviation}}{\text{average value}}\right)$

	dynamic mode				static mode			
	PP\g	PA\g	PA\c	PA\k	PP\g	PA\g	PA\c	PA\k
Long	6.8	3	not available	2.4	6	6.2	8.6	23.6
Trans	10	4	17.5	11.1	26.1	7.9	18.1	5.6

TABLE 5. Coefficient of variation (%) of K_{Ic} on the 10 mm fibre reinforced composites (high deformation speed). The coefficient of variation is defined as $\left(\frac{100 * \text{standard deviation}}{\text{average value}}\right)$

	dynamic mode				static mode			
	PP\g	PA\g	PA\c	PA\k	PP\g	PA\g	PA\c	PA\k
Long	8.9	18.3	11.1	9.7	9.1	22	15	17.4
Trans	7.7	5.9	30.2	11.1	3.9	8	11.3	7.8

of PP\g 10 and PA\g 10 are shown in figure 1. In figure 1 the value 0 for the position corresponds to the centre of the plaque, whereas the positions -42.5 mm and 42.5 mm refer to the extremities of the plaque with dimensions 85 x 85 mm. For the glass fibre composites, the modulus taken in the transverse direction seems to be independent of the position of the test specimen in the plaque. For the longitudinal direction a parabolic profile is found with an extreme in the centre plane (position = 0). Whilst the parabola shows a minimum for the STATIC mode, a maximum occurs in the DYNAMIC mode.

Plaque to plaque variations are another source of scatter in the values reported by the individual laboratories. For the tensile modulus of PA\c 10 a coefficient of variation of 27 % has been found for samples cut in the longitudinal direction at the centre of the plaques.

The variations described were likely to be related to an inhomogeneous microstructure in the plaques. This was confirmed by the structural and rheological studies (references 3 and 5) where it was observed that for these materials fibre segregation caused the plaques' extremities to have a higher fibre contents than the rest of the plaque. It has also been noted that the long fibres induced a large melt elasticity which gave rise to melt memory effects in the flow channels. This produced a tendency for the melt to foam in divergent flow-fields, maybe giving rise to voids. The long fibre aspect-ratio seemed to make the material flow as bundles of fibres, even though the fibres were wetted by the polymer, with the resultant microstructure having a domain characteristic. The microstructure was therefore position dependent: the fibre content and the fibre orientation varied from one position in the plaque to another.

Due to the heterogeneity the plaques must be seen as a structure rather than a material. The complicated anisotropic structure yielded properties which were strongly influenced by the position of the test specimen. The values presented for the mechanical properties reflect the complexity of this structure. The following format will be used to present the data: P_{MIN}/P_{MAX}, with P_{MIN} being the minimum value quoted by the participating laboratories and P_{MAX} the maximum value. P_{MIN} and P_{MAX} are the average values for the properties measured on test specimens taken from different positions in the plaque. The difference P_{MAX}-P_{MIN} reflects the between-plaque variation and the standard deviations on P_{MIN} and P_{MAX} relate to the heterogeneity of the mouldings.

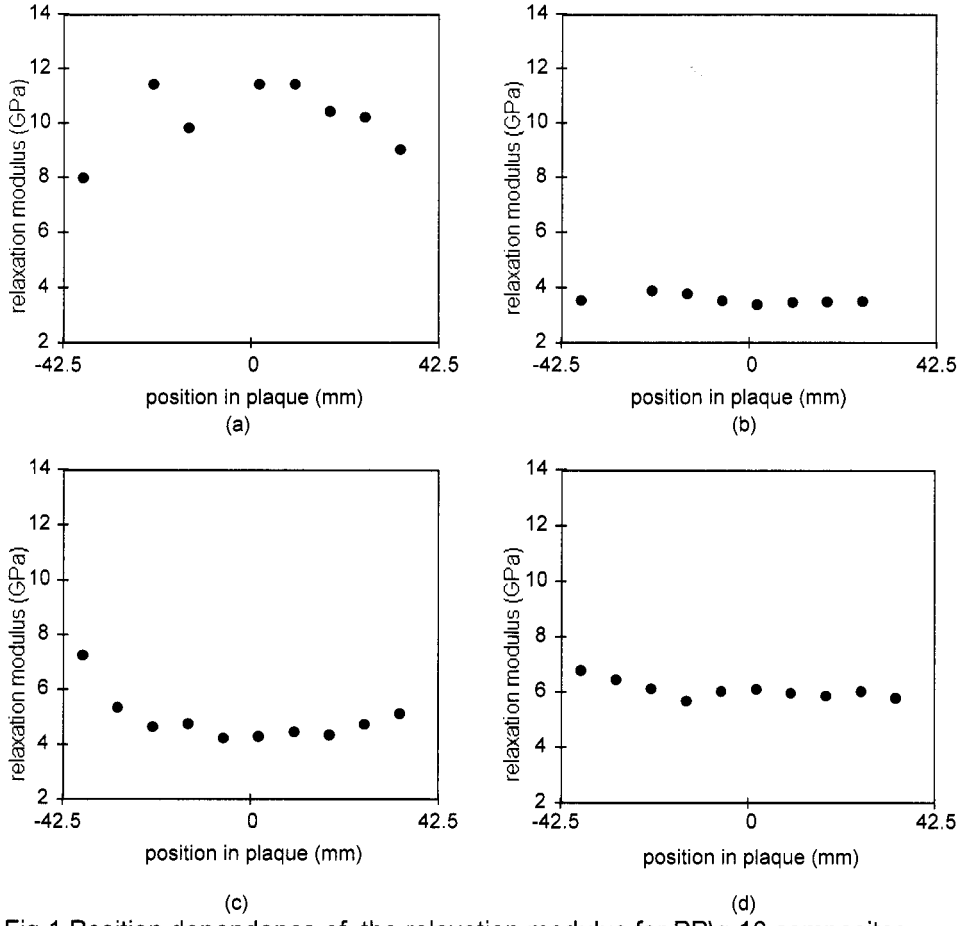

Fig 1 Position dependence of the relaxation modulus for PP\g 10 composites,
(a) dynamic mode - longitudinal direction, (b) dynamic mode - transverse direction
(c) static mode - longitudinal direction, (d) static mode - transverse direction

Initial fibre length

Tables 6, 7 and 8 present an overview of properties measured on the PP\g and PA\g composites with feedstock fibre length of 5 and 10 mm. Within the experimental variation, the properties of the composites based on 5 mm feedstock fibre length and those based on 10 mm feedstock fibre length are the same. Changing the initial feedstock fibre length did not change the mechanical properties of the composites.

TABLE 6. Tensile modulus data (GPa) for PP and PA composites (low deformation speed)

	dynamic mode				static mode			
	PP\g 5	PP\g 10	PA\g 5	PA\g 10	PP\g 5	PP\g 10	PA\g 5	PA\g 10
Long	9.3/13.6	10.1/13.8	11	10/11.8	3.9/5	4.2/5.9	8.8	7.8/8.9
Trans	3.4/4.6	3.7/4.2	6.2	6.1/6.3	6.1/8	6.1/7.9	11.9	11

TABLE 7. Ultimate strength (MPa) for PP and PA composites (low deformation speed)

	dynamic mode				static mode			
	PP\g 5	PP\g 10	PA\g 5	PA\g 10	PP\g 5	PP\g 10	PA\g 5	PA\g 10
Long	49/54	57	129/133	113/133	39/48	47/51	75/88	84/86
Trans	17/19	16/18	62/67	49/46	60/66	66/73	147/155	133/163

TABLE 8. K_{Ic} (MPa.√m) for PP and PA composites (low deformation speed)

	dynamic mode				static mode			
	PP\g 5	PP\g 10	PA\g 5	PA\g 10	PP\g 5	PP\g 10	PA\g 5	PA\g 10
Long	3.2	2.8/3	6/7.2	5.9/7	2.7/2.8	3.6/3.7	4.3/4.6	4.2/5.5
Trans	1.3/1.5	1.3/2.1	3.7/4.3	3.7/6	4.8/4.9	5/5.3	8.3/8.6	7.8/8.1

Fibre length distributions for the PP\g composites (reference 3) have shown that for a given processing mode the fibre length distributions measured on the 5 mm and 10 mm composites are almost identical. Theoretical models by Cox (ref. 11) and Kelly (ref. 12) show the modulus and the strength to depend on a critical fibre length, for a given fibre orientation and a given matrix. Similar observations have been made for fracture toughness (ref. 13). Assuming that the processing mode does not influence the state of the fibre-matrix interfacial characteristics, the lack of differences in PP\g composite moulding performance for different initial feedstock fibre lengths can therefore be attributed to the higher degree of fibre attrition of the 10 mm fibres in the two injection moulding processes. This effect is also valid for the PA\g composites where it was found that for a given processing mode the fibre length distributions of the mouldings were similar for the 5 and 10 mm original fibre lengths.

In view of these findings the composite properties will, therefore, only be reported for 10 mm fibre composites.

TABLE 9. Tensile modulus (GPa) for 10 mm fibre reinforced composites (low deformation speed)

	dynamic mode				static mode			
	PP\g	PA\g	PA\c	PA\k	PP\g	PA\g	PA\c	PA\k
Long	10.1/13.8	10/11.8	19/30	5.5	4.2/5.9	7.8/8.9	8.8/15	5
Trans	3.7/4.2	6.1/6.3	8.6/12.3	4.8	6.6/7.9	11.1	19/24	7

OVERVIEW OF THE MECHANICAL PROPERTIES

Tensile properties: modulus and ultimate strength

Table 9 presents the tensile modulus data at low deformation speeds (0.1-1 mm/min). In the longitudinal direction of the plaques produced by the DYNAMIC mode, where fibre alignment is maximal, the fibre type dominates the tensile modulus, as shown by the similarity of data for the PP\g and PA\g composites and the significantly higher modulus for the carbon fibre reinforced PA. The PA\k material has rather poor properties, probably due to the chaotic mould filling process, the random fibre orientation and poor fibre/matrix bonding. For the STATIC mode and the transverse direction of the DYNAMIC mode, the tensile modulus varies both with fibre type and matrix.

In high speed experiments (0.1 m/s) the dominating effect of the fibre type on the tensile modulus in the direction of maximum degree of fibre orientation has disappeared. The replacement of the PP matrix by a PA matrix in the glass fibre composites gave a significant increase in modulus (table 10).

TABLE 10. Tensile modulus (GPa) for 10 mm fibre reinforced composites (high deformation speed)

	dynamic mode				static mode			
	PP\g	PA\g	PA\c	PA\k	PP\g	PA\g	PA\c	PA\k
Long	7.3	15.1	31.4	8.3	5	8.1	13	5.5
Trans	2.9	4.5	11.3	5.3	5.4	10.6	31	7.1

TABLE 11. Ultimate strength (GPa) in tension for 10 mm fibre reinforced composites (low deformation speed)

	dynamic mode				static mode			
	PP\g	PA\g	PA\c	PA\k	PP\g	PA\g	PA\c	PA\k
Long	57	113/133	118/140	65/67	47/51	84/86	43	99
Trans	16/18	46/49	47/52	46/49	66/73	133/163	153	70

TABLE 12. Ultimate strength (GPa) in tension for 10 mm fibre reinforced composites (high deformation speed)

	dynamic mode				static mode			
	PP\g	PA\g	PA\c	PA\k	PP\g	PA\g	PA\c	PA\k
Long	88	153	159	72	81	112	101	68
Trans	31	77	93	59	105	183	180	100

TABLE 13. Matrix-fibre properties for 10 mm fibre reinforced composites

	Interfacial shear strength (MPa)	fibre pull-out length (mm)
PP\g	5.0	3.25
PA\g	27.3	0.62
PA\c	49	0.1

In the DYNAMIC mode the ultimate strength (tables 11 and 12) of the glass fibre reinforced PA composite is almost identical to the ultimate strength of the carbon fibre reinforced PA material, whereas the PP\g composite has a significantly lower ultimate strength. Moreover the values for the ultimate strength in the transverse direction of the STATIC mode, are higher than the ultimate strength values obtained in the longitudinal direction of the DYNAMIC mode. In the first instance this observation relates the ultimate strength solely with the nature of the matrix, and not with the nature of the fibre and the matrix-fibre interaction.

For the PA\c and PA\g systems, table 13 presents data from laboratory 4 on interfacial shear strength determined in fibre pull-out tests, and critical fibre lengths measured by fractography. The higher interfacial shear strength of the PA\c composite compared to the PA\g composite is not reflected in a higher ultimate stress. The ultimate strength of this type of composite has been modelled (ref. 14) with the following equation, based on the shear-lag assumption:

$$\sigma_c = \eta_0 \sum_{l_i < l_c} \frac{\tau l_i V_i}{2r} + \eta_0 \sum_{l_j > l_c} \sigma_f V_j \left(1 - \frac{l_c}{2 l_j}\right) + \sigma_m (1 - V_f)$$

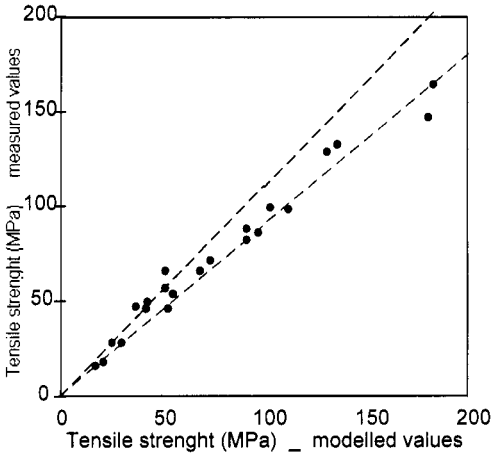

Fig. 2 Experimental versus modelled values of tensile strength

in which τ is the interfacial shear strength (measured via fibre pull out tests), r is the fibre radius, l_c is the critical fibre length (obtained by fractography), l_i and l_j are the actual fibre lengths below and above l_c respectively (determined via fibre length distributions), V_i and V_j are the corresponding fibre volume fractions, σ_f is the fibre strength, σ_m is the stress in the matrix at the fracture strain of the fibre, V_f is the total fibre volume fraction and η_0 the apparent orientation factor or degree of fibre misalignment which can be deduced from a modified rule of mixtures for the tensile modulus.

A comparison between measured and modelled data is shown in figure 2. Practically all calculated data lie within a drawn +/- 10 % band of the experimental values. The model shows that the nature of the matrix is not the only factor contributing to the ultimate stress. It also shows that the influence of the matrix-fibre adhesion, the type of the fibre and the fibre orientation can be masked by differences in the underlying fibre length distributions.

Modulus by flexure

Considering the differences in skin core morphology obtained for the samples manufactured by the DYNAMIC and STATIC mode, and the nature of the flexural tests, it was expected that the edgewise and flatwise measured rebound moduli (tables 14 and 15) would be significantly different. However, this effect has not been observed. From the data available it is not possible to explain this lack of differences.
At low deformation speeds (table 16) the effect of fibre type on the modulus by flexure is comparable to what has been found for the tensile modulus.

Fracture toughness

The observations for K_{Ic} (table 17) are very similar to those made for the ultimate stress. The higher fibre alignment in the longitudinal direction of the plaques produced by the DYNAMIC mode is not reflected in a higher K_{Ic} value for these plaques. The highest K_{Ic} values are found in the transverse directions of the plaques produced by the STATIC mode.

TABLE 14. Flatwise rebound modulus by flexure (GPa) for 10 mm fibre reinforced composites

	dynamic mode				static mode			
	PP\g	PA\g	PA\c	PA\k	PP\g	PA\g	PA\c	PA\k
Long	11.1	12.1	26.1	8	7.4	10.3	17.7	7
Trans	4.7	7.2	12.8	6	7	9.2	19.3	7

TABLE 15. Edgewise rebound modulus by flexure (GPa) for 10 mm fibre reinforced composites

	dynamic mode				static mode			
	PP\g	PA\g	PA\c	PA\k	PP\g	PA\g	PA\c	PA\k
Long	7.9	11.3	27.1	7	5.8	8.4	15.8	6
Trans	4.8	7.4	11.6	6	6.9	9.9	26.7	7.4

TABLE 16. Modulus by flexure (GPa) for 10 mm fibre reinforced composites (low deformation speeds)

	dynamic mode			static mode		
	PP\g	PA\g	PA\c	PP\g	PA\g	PA\c
Long	8.6	9.7	13	4.8	7.4	8.8
Trans	5.9	5.7	5.6	6.9	7.2	12.1

TABLE 17. K_{Ic} (MPa.√m) for 10 mm fibre reinforced composites (high deformation speed)

	dynamic mode				static mode			
	PP\g	PA\g	PA\c	PA\k	PP\g	PA\g	PA\c	PA\k
Long	5.6	8.2	8.1	3.6	5.5	8.2	6	4.6
Trans	2.6	3.4	4.3	2.9	7.7	12.5	9.7	6.4

K_{Ic} has been related with ultimate stress through following equation:

$$K_{Ic} = Y\sigma\sqrt{a}$$

where Y is a geometrical factor and a is the critical crack length or flaw size. When plotting this relation (figure 3) it is shown that the critical defect size is a constant for a given processing mode and does not depend on the nature of the individual constituents. Furthermore the linear relation between K_{Ic} and the ultimate stress indicates that the material variables that determine the ultimate stress, will also determine the fracture toughness. The lower slope for the materials processed by the DYNAMIC mode indicates that the critical defect size is smaller for this processing route. The smaller critical flaw size is possibly related to the higher degree of fibre attrition and therefore a statistically higher chance for a defect site with the DYNAMIC mode.

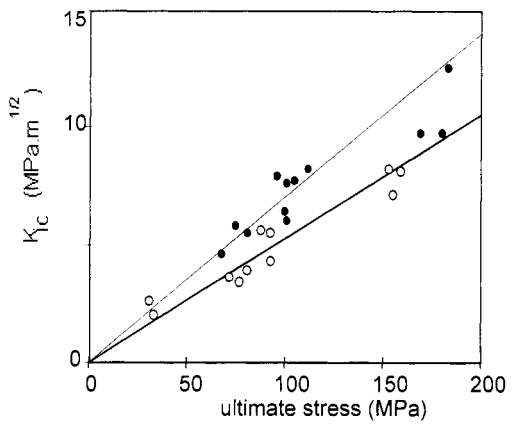

Fig. 3 K_{Ic} versus the ultimate stress for samples manufactured by the DYNAMIC mode (○) and STATIC mode (●) .

Falling Weight Impact testing

A typical load deflection pattern for the instrumented falling weight impact test is shown in figure. 4. Failure occurred in two steps, similar to that which was reported for PEEK by laboratory 3 in a previous IUPAC 4.2.1 Working party project (reference 15). After some initial oscillation due to inertial effects occurring on impact, the load increases up to the point where first damage (crack initiation) occurs. The force and energy values recorded at this point are given in table 18. This table also contains the energy at rupture, although it is recognised that rupture data can be questioned because the energy at rupture is influenced by other effects than crack propagation only.

TABLE 18. Instrumented falling weight impact results on plaques for 10 mm fibre reinforced composites.

	dynamic mode			static mode		
	force at first damage (N)	energy at first damage (J)	energy at rupture (J)	force at first damage (N)	energy at first damage (J)	energy at rupture (J)
PP\g	1538	1.4	10.6	2802	3.7	37
PA\g	2075	1.9	13.6	3727	4.9	39.3
PA\k	1612	1.6	6.7	2195	2.4	19.8

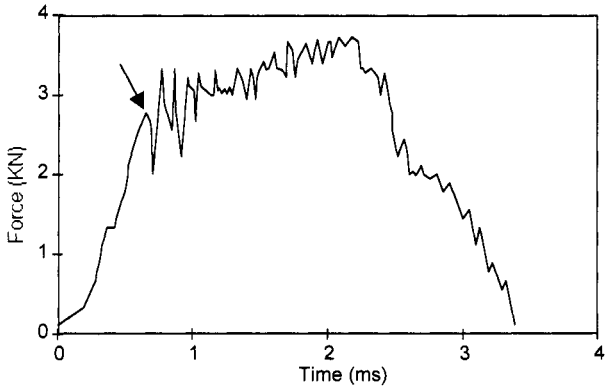

Fig. 4 Typical force versus time signal for instrumented falling weight impact on a PP\g 10 composite. The arrow indicates the force/time where the crack initiates.

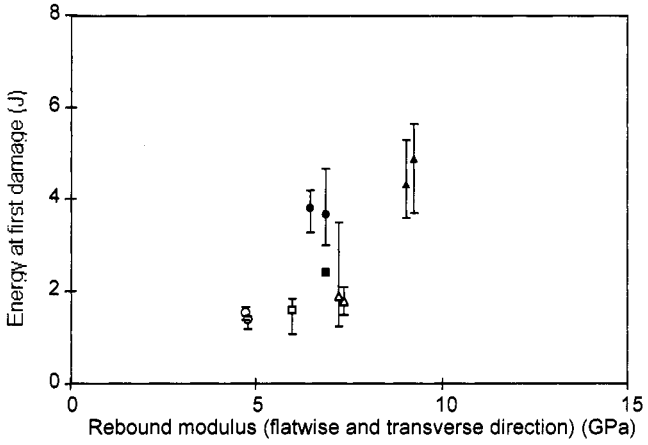

Fig. 5. Energy at first damage versus flatwise rebound modulus (transverse direction) for 10 mm fibre reinforced composites. O● PP\g, □■ PA\g, Δ ▲ PA\k.
O□Δ: samples manufactured by the DYNAMIC mode. ● ■ ▲:samples manufactured by the STATIC mode. The bar denotes the experimental variation of the energy at first damage.

A good correlation between the energy at first damage and the flatwise rebound modulus (figure 5) indicates the importance of fibre orientation for this property. For this correlation the flatwise rebound modulus was used in view of the similarity with the geometry of the falling dart test. The influence of processing mode on impact properties is shown by the correlation between the force at first damage and the fracture toughness (figure 6). It is observed that data measured on plaques produced by the DYNAMIC mode lie on the lower portion of the line, whereas the data pertaining to the STATIC mode lie on the upper part.

The events occurring during a falling weight disk impact are known to involve a wide range of micro-mechanical deformations (elastic, plastic, fibre pull-out..) and the correlations presented here indicate that these type of properties are related to fibre orientation and skin morphology (flatwise rebound modulus), fibre attrition (processing mode) and matrix fibre-interface (fracture toughness).

Tensile creep

Figure 7 presents some creep data for the PP\g 10 composite. The higher modulus specimens (cut from the longitudinal direction of the plaques produced by the DYNAMIC mode, the transverse direction for the STATIC mode) showed the lowest time-dependence despite being tested at much higher stress levels.

Relaxation modulus

Temperature dependence of the relaxation modulus of the PP\g composites is shown in figure 8. With increasing temperature a reduction in stiffness is observed. This softening is accompanied by an increased anisotropy in relaxation modulus. Figure 8 also shows that there is less softening for the plaques produced by the STATIC mode than for the plaques produced

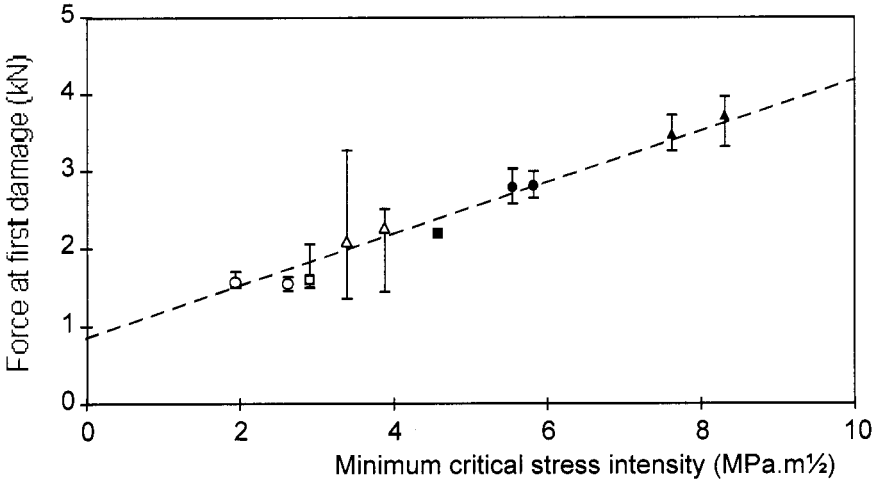

Fig. 6 Force at first damage versus minimum K_{Ic} for 10 mm fibre reinforced composites.○● PP\g, □■ PA\g, Δ ▲ PA\k .
○□Δ: samples manufactured by the DYNAMIC mode. ● ■ ▲samples manufactured by the STATIC mode. The bar denotes the experimental variation of the force at first damage.

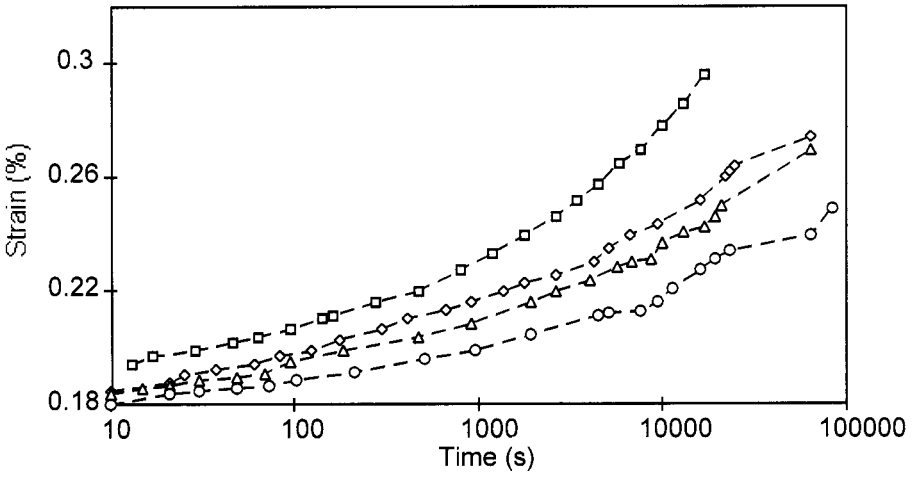

Fig. 7 Tensile creep data for PP\g 10 at 25°C.
□ : samples manufactured by the DYNAMIC mode, loaded in the transverse direction with a creep stress of 6.8 MPa;
◊: samples manufactured by the STATIC mode, loaded in the longitudinal direction with a creep stress of 8 MPa;
Δ: samples manufactured by the DYNAMIC mode, loaded in the longitudinal direction with a creep stress of 20 MPa
○: samples manufactured by the STATIC mode, loaded in the transverse direction with a creep stress of 12.3 MPa

by the DYNAMIC mode. Annealing of the samples prior to measuring the relaxation modulus or changing the strain level at which the relaxation modulus was measured, did not influence the results.

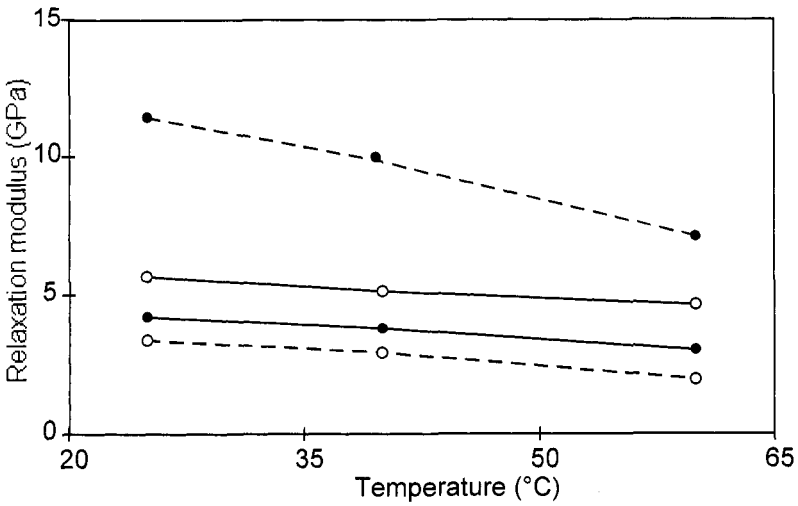

Fig. 8 Temperature dependence of the relaxation modulus for PP\g composites. Dotted lines are for samples manufactured by the DYNAMIC mode. Full lines are for samples manufactured by the STATIC mode.
● : properties measured in the transverse direction,
○ properties measured in the longitudinal direction.

CONCLUSIONS

♦ Simple plaques manufactured by injection moulding of finite length fibre reinforced thermoplastics exhibit complicated heterogeneous structures. The properties of such materials are highly dependent on the position of the test specimen in the plaque. Consequently the measured properties are not representative of the 'material aspects' of the constituents and their concentrations; but are more a complex response of a strongly anisotropic structure.

♦ Differences in feedstock fibre length do not influence mechanical properties of the composites. Due to fibre attrition during moulding, the fibre length distribution in the composite is the same, regardless of the feedstock length.

♦ Increased fibre orientation, as obtained by multiple live feed moulding, is accompanied by an increase in tensile modulus. In the direction of highest fibre alignment the modulus is controlled by the fibre type.

♦ The higher level of unidirectional fibre alignment induced by the multiple-live feed process did not produce the expected increase in the ultimate strength and fracture toughness. The nature of the more ordered fibre structure and the shorter fibre length produced by the live-feed process are believed to be the main contributing factors to this effect

♦ Several correlations have been presented between a range of properties, such as fracture toughness, flatwise rebound modulus and instrumented impact.

REFERENCES

1. A. Cervenka and P.S. Allan: Characterization of finite length fibre composites Part I: Introductory paper, Pure Appl. Chem., submitted for publication.

2. .A. Cervenka, G. Ajroldi, F.H.J. Maurer and P.S. Allan: Characterization of finite length fibre composites Part III: Studies thin sections extracted from mouldings (wafers), Pure Appl. Chem., submitted for publication.

3. G. von Bradsky, R.S. Bailey, A. Cervenka and P.S. Allan: Characterization of finite length fibre composites Part IV: Determination of structural aspects of composites, Pure Appl. Chem., submitted for publication.

4. P.S. Allan, A. Cervenka and D.R. Moore: Characterization of finite length fibre composites Part V: Modelling of stiffness, Pure Appl. Chem., submitted for publication.

5. R.S. Bailey and D.J. Groves: Characterization of finite length fibre composites Part VI: Rheological studies of materials based on the polypropylene matrix, Pure Appl. Chem., submitted for publication.

6. ASTM D790, Test methods for flexural properties of unreinforced and reinforced plastics and electrical insulating materials.

7. T. Casiraghi, Polym. Eng. Sci 23, 16 (1983).

8. ASTM D256, Standard test methods for determining the pendulum impact resistance of notched specimens of plastics.

9. T. Casiraghi, G. Castiglioni, Materie Plastiche ed Elastomeri (1976) 765.

10. ASTM E399, Test methods for plane-strain fracture toughness of metallic materials.

11. H.L. Cox, Brit. J. Physics 3 (1952) p72.

12. A. Kelly and N.M. MacMillan, "Strong solids", Clarendon Press, Oxford, 1986.

13. D.W. Clegg and A.A. Collyer, "Mechanical properties of reinforced thermoplastics", Elsevier Applied Science Publishers, 1986.

14. T.Vu-Khanh, J. Denault, P. Habib and A. Low, Comp. Sci. Techn., 40, 423, (1991).

15. D.R. Moore and J.C. Seferis, "Intrinsic characterization of continuous fibre reinforced thermoplastic composites - I: Toughness characterization of carbon fibre/polyether ether ketone (CFPEEK) laminates, Pure & Appl. Chem., Vol. 63, No. 11, pp 1609-1625, (1991).